HHS Public Access

Author manuscript

J Med Chem. Author manuscript; available in PMC 2018 August 24.

Published in final edited form as:

J Med Chem. 2018 August 09; 61(15): 6748–6758. doi:10.1021/acs.jmedchem.8b00566.

Discovery of a Potent, Selective, and Brain-Penetrant Small Molecule that Activates the Orphan Receptor GPR88 and Reduces Alcohol Intake

Chunyang Jin[*,†], **Ann M. Decker**[†], **Viren H. Makhijani**[‡], **Joyce Besheer**[‡,#], **Emmanuel Darcq**[§], **Brigitte L. Kieffer**[§], and **Rangan Maitra**[†]

[†]Center for Drug Discovery, Research Triangle Institute, Research Triangle Park, North Carolina 27709, United States

[‡]Bowles Center for Alcohol Studies, University of North Carolina at Chapel Hill, Chapel Hill, North Carolina 27599, United States

[#]Department of Psychiatry, University of North Carolina at Chapel Hill, Chapel Hill, North Carolina 27599, United States

[§]Department of Psychiatry, Douglas Mental Health Research Institute, McGill University, Montreal, Quebec H4H 1R3, Canada

Abstract

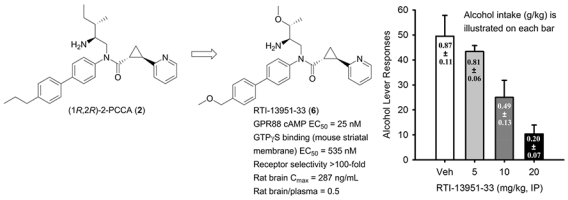

The orphan G-protein-coupled receptor GPR88 is highly expressed in the striatum. Studies using GPR88 knockout mice have suggested that the receptor is implicated in alcohol seeking and drinking behaviors. To date, the biological effects of GPR88 activation are still unknown due to the lack of a potent and selective agonist appropriate for in vivo investigation. In this study, we report the discovery of the first potent, selective, and brain-penetrant GPR88 agonist RTI-13951-33 (**6**). RTI-13951-33 exhibited an EC_{50} of 25 nM in an in vitro cAMP functional assay and had no significant off-target activity at 38 GPCRs, ion channels, and neurotransmitter transporters that were tested. RTI-13951-33 displayed enhanced aqueous solubility compared to

[*]**Corresponding Author**: Phone: 919 541-6328. Fax: 919 541-8868. cjin@rti.org. Address: Research Triangle Institute, PO Box 12194, Research Triangle Park, North Carolina 27709, United States. .

Supporting Information

The Supporting Information is available free of charge on the ACS Publications website at DOI: 10.1021/acs.jmedchem.8b00566. HPLC analysis of **4c**, **4f**, **4h**, **5a**, **5b**, and **6**, and the full report for off-target radioligand binding profile (PDF) Molecular formula strings with biological data (CSV)

Author Contributions

The manuscript was written through contributions of all authors. All authors have given approval to the final version of the manuscript.

The authors declare no competing financial interest.

(1*R*,2*R*)-2-PCCA (**2**) and had favorable pharmacokinetic properties for behavioral assessment. Finally, RTI-13951-33 significantly reduced alcohol self-administration and alcohol intake in a dose-dependent manner without effects on locomotion and sucrose self-administration in rats when administered intraperitoneally.

INTRODUCTION

Alcohol use disorders (AUDs) remain a significant clinical problem and exact great emotional, social, and economic costs.[1,2] It is well-known that alcohol interacts with a number of neurotransmitters in the brain and triggers broad alterations in gene expression and synaptic plasticity.[3–6] In regard to the brain reward system, alcohol affects both the dopamine and opioid systems.[4] Accordingly, the competitive opioid antagonist naltrexone and the functional glutamate receptor antagonist acamprosate have been approved by the U.S. Food and Drug Administration to treat alcoholism.[7] However, both drugs face significant challenges including lack of adherence, low efficacy, and serious side effects.[7–10] In addition, alcoholism is a heterogeneous disorder and there is no single effective treatment for all alcoholic patients.[10] Therefore, new therapeutic agents based on novel targets are urgently needed.

GPR88 is an orphan G-protein-coupled receptor (GPCR) and has a high expression in both dorsal and ventral areas of the striatum.[11,12] GPR88 has also been found in other regions of the brain, including the cerebral cortex, amygdala, and hypothalamus.[13–17] In the striatum, GPR88 is expressed at postsynaptic sites in medium spiny neurons (MSNs) of both direct and indirect pathways.[15] A number of studies using GPR88 knockout (KO) mice have suggested that genetic ablation of GPR88 induces a state of hypersensitivity to the dopamine system, and the receptor is implicated in disease states such as schizophrenia and anxiety.[18–22] Interestingly, a recent GPR88 KO study demonstrated that the GPR88-deficient mice displayed enhanced voluntary alcohol drinking in both moderate and excessive drinking paradigms compared with wild-type (WT) mice.[23] No alterations in water intake, palatability, and alcohol metabolism were observed in these mice.[23] Moreover, mice lacking the GPR88 gene showed enhanced motivation for alcohol drinking and seeking behaviors using operant self-administration.[23] Altogether, these findings suggest that weak GPR88 signaling may represent a vulnerability factor for AUDs and GPR88 might serve as a novel drug target to treat AUDs.

We have previously reported that GPR88 is a $G\alpha_i$-coupled GPCR activated by a synthetic agonist, 2-PCCA (**1**, Figure 1).[24] Unfortunately, 2-PCCA is expected to have poor brain bioavailability due to its high lipophilicity (clogP 6.19) and its activity as a substrate of P-glycoprotein.[25] Thus, an improved agonist probe is required to elucidate the in vivo functions of GPR88. Structure–activity relationship (SAR) studies from our laboratory, as well as others, have focused on sites A–C of 2-PCCA and determined a preliminary understanding of receptor tolerances at each site (Figure 1).[24–27] For example, the aromatic ring on site A is essential for activity but has limited substitution tolerance, suggesting the binding space around this region is constrained. The (1*R*,2*R*)-*trans* configuration of the cyclopropane linkage is more potent than the (1*S*,2*S*)-*trans* and *cis*-isomers. On site B, the

4′-position of the biphenyl ring is well tolerated with small- to large-sized alkyl or alkoxy groups, which likely exits through a hydrophobic binding pocket to the extracellular loop consistent with a binding position in the GPR88 homology model. On site C, the (*S*)-amino group is important for potency. We previously demonstrated that the ethylamine moiety of site C had tolerance for modification.[24] In this study, we continued to investigate SAR at site C and tested a series of analogues (**4a–h**, Figure 2) bearing small- to large-sized amino alkyl side chains with the goal of improving potency and drug-like properties for brain penetration. We then combined the positive SAR results obtained from sites A–C and designed analogues **5a** and **5b**, which led to the discovery of the first potent, selective, and brain-penetrant small molecule **6** (designated as RTI-13951-33) that activated GPR88 and significantly reduced alcohol reinforcement and intake behaviors in rats.

RESULTS AND DISCUSSION

Synthesis.

The overall synthetic approach followed methods detailed in our earlier publications.[24,27] Synthesis of compounds **4a–g** is shown in Scheme 1. Reductive amination of an appropriate aldehyde **7a–g** with 4-bromoaniline (**8a**) or 4-(4′-propylphenyl)aniline (**8b**) using sodium triacetoxyborohydride in 1,2-dichloroethane afforded amine **9a–g** in 50–86% yields. Reaction of **9a–g** with the acid chloride of racemic (±)-*trans*-2-(pyridin-2-yl)cyclopropanecarboxylic acid gave amide **10a–g** in 49–60% yields. Suzuki coupling of **10a**, **10b**, and **10g** with 4-propylphenylboronic acid under microwave conditions yielded 53–80% of **11a**, **11b**, and **11g**. Removal of the Boc group with 4 M HCl in dioxane furnished **4a–g** in 92–98% yields.

Synthesis of the (*R*)-1-methoxyethyl derivatives **4h**, **5a**,**b**, and **6** is outlined in Scheme 2. HBTU-assisted amide coupling between 4-bromoaniline (**8a**) and *N*-Boc-*O*-methyl-L-threonine (**12**) led to **13**, which was subsequently reduced with borane in THF to give amine **14** in 31% yield over two steps. Amide formation afforded **15** in 95% yield. Suzuki coupling of **15** with arylboronic acid, followed by Boc deprotection, provided **4h** and **5a,b** in the range of 62–77% yields. Target compounds **4b**, **4d–h**, and **5a,b** were 1:1 mixtures of (1*R*,2*R*)- and (1*S*,2*S*)-enantiomers, differentiating at the configuration of the *trans*-substituted cyclopropane, determined by ^{1}H NMR and HPLC analyses. The pure diastereomer **6** was synthesized using the procedure analogous to that used to prepare (1*R*,2*R*)-2-PCCA.[24] The 1:1 diastereomeric mixture **15** was separated by a chiral HPLC, affording (1*R*,2*R*)-**15** and (1*S*,2*S*)-**15** (structure not shown) in 48% and 47% yield, respectively. The configuration of (1*R*,2*R*)-**15** was assigned based on the comparison of its ^{1}H NMR spectrum and HPLC retention time with those of a sample synthesized from pure (1*R*,2*R*)-2-(pyridin-2-yl)cyclopropanecarboxylic acid.[24] Finally, Suzuki coupling with 4-(methoxymethyl)phenylboronic acid, followed by Boc deprotection, provided RTI-13951-33 (**6**) in 64% yield.

Pharmacological Evaluations.

We previously examined a brief SAR on site C of 2-PCCA in a GloSensor cAMP assay using stable HEK293-GPR88-pGloSensor22F cells.[24] Later, we observed that, over time, the

HEK293 cells were physically unhealthy after transfection with GPR88 and subsequently led to deteriorated responses to 2-PCCA.[26] To facilitate the SAR study, we recently created a stable CHO-PPLS-HA-GPR88 cell line and measured cAMP levels using the PerkinElmer Lance assay kit.[27] The new assay system is reliable and sensitive and therefore was used in subsequent SAR studies.

Our efforts on the optimization of 2-PCCA have focused on improving its brain permeability by lowering the lipophilicity while retaining or enhancing potency. Early SAR studies suggest that the substituted ethylamine moiety on site C is suitable for modification. In the present study, we further explored the SAR on this site and evaluated a series of analogues **4a–h** in the GPR88 Lance cAMP assays. The results are presented in Table 1. The unsubstituted analogue **4a** was approximately 4-fold less potent than 2-PCCA (501 vs 126 nM). Addition of a methyl group (**4b**) or 1,1′-dimethyl groups (**4c**) slightly improved potency with EC_{50} values of 398 and 316 nM, respectively. The potency was further improved by adding a medium-sized alkyl side chain with the isobutyl analogue **4e** (EC_{50} = 126 nM) being equipotent to 2-PCCA. Interestingly, substitution with a phenyl group (**4f**) led to a significant loss of potency (EC_{50} = 1260 nM), whereas the phenylmethyl analogue **4g** retained a moderate activity. Further optimization of the amino alkyl side chain of 2-PCCA by inserting an oxygen to lower lipophilicity gave **4h** with an EC_{50} value of 63 nM. In general, a medium-sized alkyl side chain is well tolerated on site C, indicating a hydrophobic binding pocket for this region. An alkoxy group can also be tolerated on this site to further enhance potency and lower lipophilicity.

With the positive SAR results obtained on site C, we next combined our optimized biphenyl substitution (site B) with the amino alkyl side chain (site C) in an effort to further improve the drug-like properties for CNS penetration (in general, CNS drugs have clogP = 2–4[28]) while retaining the potency. Because compound **3** (Figure 1) showed comparable potency but has lower lipophilicity than (1*R*,2*R*)-2-PCCA (**2**) (clogP 4.63 vs 6.19),[27] we designed and synthesized analogues **5a,b** with a methoxy or a methoxymethyl group on the biphenyl ring, respectively. Both compounds had good agonist activity, with **5b** (clogP = 3.34, EC_{50} = 100 nM) being slightly more potent than **5a**. Finally, we synthesized **6**, a pure (1*R*,2*R*)-diastereomer of **5b**, which had an EC_{50} of 25 nM.

Physicochemical Properties and In Vitro ADME Studies.

Physiochemical properties, such as lipophilicity (clogP), topological polar surface area (TPSA), and log BB, of select compounds (**2**, **3**, **4h**, and **6**) were calculated to predict the compound's potential for brain penetration. In general, CNS drugs have clogP of 2–4,[28] TPSA < 76 $Å^2$,[29] and log BB > −1.[30] As shown in Table 2, (1*R*,2*R*)-2-PCCA (**2**) has the highest clogP value of 6.19, whereas RTI-13951–33 (**6**) has the lowest clogP = 3.34. All compounds, except **6**, have TPSA < 76 $Å^2$. Compound **6** has a TPSA value of 77.68 $Å^2$ that is just above the recommended threshold. A TPSA cutoff of 90 $Å^2$ has also been suggested for CNS drugs.[31] Allcompounds have log BB > −1, suggesting that these compounds have the potential to penetrate the brain.

The brain permeability of select compounds were further tested in vitro using the MDCK cell line expressing the human P-glycoprotein efflux transporter. In general, compounds that have >10% permeability (expressed as % transported from apical A to basal B) in the MDCK assay are considered desirable. Only compound 6 had >10% permeability, whereas **2**, **3**, and **4h** had 1%, 8%, and 3%, respectively, with **2** being the least permeable in this series. The permeability correlated well with clogP. The solubility of select compounds was determined using a thermodynamic solubility assay. RTI-13951-33 (**6**) was highly soluble in aqueous solutions with a thermodynamic solubility of 984 ± 9.4 μg/mL (mean ± %CV) in the phosphate-buffered saline (PBS) solution. On the other hand, (1*R*,2*R*)-2-PCCA (**2**) had a much lower solubility of 46.1 ± 1.8 μg/mL, which is expected due to its high lipophilicity.

Receptor Selectivity.

The on-target activity of (1*R*,2*R*)-2-PCCA (**2**) and RTI-13951-33 (**6**) was determined in the [^{35}S]-GTPγS binding assay using striatal membrane preparations from WT mice and GPR88 KO mice. RTI-13951-33 increased [^{35}S]-GTPγS binding (EC_{50} = 535 nM) in mouse striatal membranes but not in membranes from GPR88 KO mice even at a concentration of 100 μM, indicating the compound has a GPR88-specific agonist signaling activity in the striatum (Figure 3A). By contrast, (1*R*,2*R*)-2-PCCA had an EC_{50} of 1140 nM in the WT mouse striatal membranes but also had a significant [^{35}S]-GTPγS binding at 10 μM in GPR88 KO mouse striatal membranes (Figure 3B). The off-target profile of RTI-13951-33 was further assessed in radioligand binding assays against a panel of 38 GPCRs, ion channels, and transporters at a single concentration of 10 μM, each in duplicate, by Eurofins PanLabs (Taipei, Taiwan). RTI-13951-33 at 10 μM showed binding activity only at the kappa opioid receptor (KOR), vesicular monoamine transporter (VMAT), and serotonin transporter (SERT), with inhibitions of 64%, 54%, and 55%, respectively (see Supporting Information for the full off-target profile report). The follow-up concentration–response assays determined that the compound had weak affinities at KOR (K_i = 2.29 μM) and VMAT (K_i = 4.23 μM) and a moderate affinity at SERT (K_i = 0.75 μM). RTI-13951-33 was then submitted to the NIMH Psychoactive Drug Screening Program (NIMH PDSP) to evaluate its functional activity at SERT. This compound had little inhibitory activity at SERT with an IC_{50} = 25.1 ± 2.7 μM in the neurotransmitter transporter reuptake inhibition assay. Taken together, RTI-13951-33 is GPR88 selective and has no significant off-target liability based on our selectivity evaluations.

Pharmacokinetic Study.

On the basis of potency, receptor selectivity, and in vitro ADME properties, RTI-13951-33 was further evaluated in a snapshot pharmacokinetic (PK) testing to assess whether this compound has sufficient brain exposure. Following an intraperitoneal (ip) dose of 10 mg/kg in rats, RTI-13951-33 was rapidly absorbed into systemic circulation, with peak plasma concentration (C_{max} = 874 ng/mL, Table 3) observed at 15 min postdose (the first sampling time point). The brain concentration peaked at 60 min with a C_{max} of 287 ng/mL then was eliminated from the brain with an apparent half-life of 87 min. The overall brain to plasma AUC ratio, as determined by $AUC_{0–inf}$ ratio, was 0.5. At 30 min, brain concentration was 242 ng/mL (527 nM), indicating that RTI-13951-33 had sufficient brain penetration for GPR88 modulation considering it has an EC_{50} of 25 nM in the cAMP functional assay.

In Vivo Activities of RTI-13951-33.

Because GPR88 KO mice showed enhanced motivation for alcohol drinking and seeking behaviors,[23] we sought to determine whether RTI-13951-33 would be effective in vivo to alter operant alcohol self-administration. Female Long Evans rats were trained to self-administer alcohol, as described in our recent publications (15% alcohol [v/v] + 2% [w/v] sucrose vs inactive lever).[32–34] This sweetened alcohol concentration was used in all of our studies because we found that it results in stable operant responding over time and allows animals to achieve physiologically relevant and moderate alcohol intake (e.g., 0.7–1.0 g/kg). A significant decrease in alcohol self-administration was observed at the two highest RTI-13951-33 doses tested (10 and 20 mg/kg, Figure 4A). This decrease in alcohol lever responses corresponded to decreased alcohol intake (g/kg) at the highest dose (20 mg/kg) and a trend for a decrease at the 10 mg/kg dose ($p = 0.05$, Figure 4A). Notably, there was no effect on inactive lever responses (mean ± SEM; vehicle, 0.8 ± 0.3; 5 mg/kg dose, 1.1 ± 0.4; 10 mg/kg dose, 0.5 ± 0.3; 20 mg/kg dose, 0.0 ± 0.0 responses) or locomotor rate (Figure 4B) measured during the self-administration sessions,[35] suggesting that the decrease in alcohol self-administration was not related to a general suppression of activity.

For a comparative assessment of actions on intake of a natural reward, a separate cohort of rats was trained to self-administer sucrose (0.8% [w/v] sucrose vs inactive lever; FR2). This sucrose concentration was chosen as it resulted in lever responding similar to the alcohol self-administration group. There was no difference in sucrose lever responses, or sucrose intake at any RTI-13951-33 dose vs vehicle (Figure 4C). Interestingly, there was a trend for a reduction in locomotor rate [$F(3,18) = 3.16$, $p = 0.05$, mean ± SEM; vehicle, 27.0 ± 1.8; 5 mg/kg dose 24.0 ± 2.0; 10 mg/kg dose 23.6 ± 1.2; 20 mg/kg dose 17.9 ± 3.6 beam breaks/min], but this did not affect sucrose lever responses. Given the lack of modulatory effect on sucrose self-administration at doses that reduced alcohol self-administration, this suggests that the compound had a selective effect for alcohol reinforcement.

CONCLUSIONS

In summary, we have developed a potent, selective, and brain-penetrant GPR88 agonist RTI-13951-33 (**6**) based on the 2-PCCA scaffold. The in vitro pharmacological evaluations revealed that RTI-13951-33 was highly potent in the GPR88 cAMP functional assay and had no significant off-target activity based upon our screening data of 38 GPCRs, ion channels, and transporters and had no agonist signaling activity in the GTPγS binding assay using GPR88 KO mouse striatal membranes. RTI-13951-33 displayed a good aqueous solubility and had favorable pharmacokinetic properties for brain-penetration. RTI-13951-33 showed significant efficacy in reducing alcohol intake in a rat model of alcohol self-administration. Importantly, there was no effect on locomotion measured during the self-administration sessions, indicating that the decrease in alcohol self-administration was not related to a general suppression of activity. Moreover, we demonstrated a specificity between alcohol and natural rewards, with GPR88 agonism reducing alcohol self-administration but not sucrose self-administration at equivalent doses, supporting a role of GPR88 signaling in the modulation of alcohol reinforcement. Further studies of RTI-13951-33 in the mouse model of alcohol drinking and seeking behaviors using both WT and GPR88 KO mice to assess the

in vivo on-target specificity are in progress. Taken together, GPR88 represents a novel drug target and should be further studied in the development of new treatments for alcohol use disorders.

EXPERIMENTAL SECTION

Chemistry.

General Methods.—Melting points were determined using a MEL-TEMP II capillary melting point apparatus and are uncorrected. Melting point of the diastereomeric mixture was not measured. Nuclear magnetic resonance (^{1}H NMR and ^{13}C NMR) spectra were obtained on a Bruker Avance DPX-300 MHz NMR spectrometer. Chemical shifts are reported in parts per million (ppm) with reference to internal solvent. ^{13}C NMR data of diastereomeric mixtures were not reported due to the complicity of the spectra. Mass spectra (MS) were run on a PerkinElmer Sciex API 150 EX mass spectrometer. HRMS spectra were run on a Waters Synapt G2 HDMS Q-TOF mass spectrometer, using electrospray ionization in positive ion mode. Analytical thin-layer chromatography (TLC) was carried out using EMD silica gel 60 F_{254} TLC plates. TLC visualization was achieved with a UV lamp or in an iodine chamber. Flash column chromatography was done on a CombiFlash Companion system using Isco prepacked silica gel columns. Unless otherwise stated, reagent-grade chemicals were obtained from commercial sources and were used without further purification. All moisture- and air-sensitive reactions and reagent transfers were carried out under dry nitrogen. Synthesis and characterization of compounds **1–3**, **4a,b**, **4d,e**, and **4g** have been previously reported.[24] All synthesized compounds were ≥95% pure as determined by HPLC analyses (see Supporting Information).

(1R*,2R*)-2-(Pyridin-2-yl)cyclopropanecarboxylic Acid (2-Amino-2-methylpropyl)-(4′-propylbiphenyl-4-yl)amide (4c).—A solution of **10c** (50 mg, 0.09 mmol) and 4 M HCl in dioxane (2 mL) in CH_2Cl_2 (5 mL) was stirred at room temperature for 6 h. The solvent was removed under reduced pressure. The resulting residue was triturated with hexanes to give **4c** dihydrochloride (45 mg, 95%) as an off-white solid: mp 158–160 °C. ^{1}H NMR (300 MHz; CD_3OD) δ 8.59 (d, J = 3.0 Hz, 1H), 8.35–8.45 (m, 1H), 7.80–7.45 (m, 8H), 7.26 (d, J = 6.0 Hz, 2H), 4.13 (d, J = 15.0 Hz, 1H), 3.98 (d, J = 15.0 Hz, 1H), 3.78–3.58 (m, 1H), 3.10–2.95 (m, 1H), 2.62 (t, J = 7.5 Hz, 2H), 2.25–2.15 (m, 1H), 2.00–1.90 (m, 1H), 1.75–1.55 (m, 2H), 1.34 (s, 6H), 0.96 (t, J = 7.5 Hz, 3H). ^{13}C NMR (75 MHz; CD_3OD) δ 174.1, 157.6, 146.5, 143.9, 143.4, 143.3, 142.5, 138.2, 130.2, 129.5, 129.2, 127.8, 125.5, 125.1, 59.6, 57.7, 38.6, 27.0, 25.6, 25.5, 24.8, 17.8, 14.0. HRMS (ESI) calcd for $C_{28}H_{33}N_3O$ $[M + H]^+$ 428.2696, found 428.2700.

(1R*,2R*)-2-(Pyridin-2-yl)cyclopropanecarboxylic Acid [(2S)-2-Amino-2-phenylethyl]-(4′-propylbiphenyl-4-yl)amide (4f).—The procedure for **4c** was followed using 50 mg (0.09 mmol) of **10f** to give 46 mg (97%) of **4f** dihydrochloride (1:1 diastereomeric mixture) as an off-white solid. ^{1}H NMR (300 MHz; CD_3OD) δ 8.50–8.38 (m, 1H), 8.15–8.05 (m, 1H), 7.65–7.30 (m, 9H), 7.25–6.98 (m, 6H), 4.65–4.45 (m, 1.5H), 4.05–3.85 (m, 1H), 3.68–3.25 (m, 0.5H), 2.90–2.82 (m, 0.5H), 2.82–2.70 (m, 0.5H), 2.52 (t,

J = 7.5 Hz, 2H), 2.05–1.95 (m, 1H), 1.88–1.70 (m, 1H), 1.68–1.45 (m, 3H), 0.86 (t, *J* = 7.5 Hz, 3H). HRMS (ESI) calcd for $C_{32}H_{33}N_3O$ $[M + H]^+$ 476.2696, found 476.2705.

(1R*,2R*)-2-(Pyridin-2-yl)cyclopropanecarboxylic Acid [(2R,3R)-2-Amino-3-methoxybutyl]-(4′-propylbiphenyl-4-yl)amide (4h).—A mixture of **15** (52 mg, 0.1 mmol), 4-propylphenylboronic acid (24.6 mg, 0.15 mmol), $Pd(dppf)Cl_2 \cdot CH_2Cl_2$ (8.7 mg, 0.01 mmol), and K_3PO_4 (76 mg, 5.4 mmol) in dimethoxyethane (1 mL) and water (0.3 mL) was heated in a sealed vessel by microwave irradiation at 160 °C for 6 min. The resulting mixture was poured into 1 N NaOH solution (5 mL) and extracted with CH_2Cl_2 (3 × 10 mL). The combined organic layers were dried (Na_2SO_4) and concentrated under reduced pressure. Flash column chromatography of the crude product on silica gel using 0–20% EtOAc in hexanes afforded intermediate *tert*-butyl [(2*S*,3*R*)-1-{(4′-propylbiphenyl-4-yl)-[(1*R**,2*R**)-2-(pyridin-2-yl)cyclopropanecarbonyl]amino}-3-methox-ybutan-2-yl]carbamate (44 mg, 79%, 1:1 diastereomeric mixture) as an oil. ^{1}H NMR (300 MHz; $CDCl_3$) δ 8.30–8.25 (m, 1H), 7.55–7.40 (m, 5H), 7.32–7.15 (m, 5H), 7.02–6.95 (m, 1H), 5.12–5.00 (m, 1H), 4.42–4.28 (m, 1H), 4.00–3.80 (m, 2H), 3.58–3.48 (m, 1H), 3.45–3.36 (m, 1H), 3.26 and 3.25 (s, 3H), 2.73–2.55 (m, 3H), 2.08–1.98 (m, 1H), 1.75–1.60 (m, 3H), 1.43 (s, 9H), 1.13 and 1.12 (2d, *J* = 6.0 Hz, 3H), 0.97 (t, *J* = 7.5 Hz, 3H). MS (ESI) *m/z* 558.5 $[M + H]^+$. The coupled product was then dissolved in CH_2Cl_2 (5 mL) and treated with 4 M HCl in dioxane (3 mL) at room temperature for 6 h. The solvent was removed under reduced pressure. The resulting residue was triturated with hexanes to give **4 h** dihydrochloride (40 mg, 96%, 1:1 diastereomeric mixture) as an off-white solid. ^{1}H NMR (300 MHz; CD_3OD) δ 8.40–8.28 (m, 1H), 8.00–7.88 (m, 1H), 7.65–7.25 (m, 8H), 7.20–7.05 (m, 2H), 4.30–4.18 (m, 0.5H), 4.18–4.06 (m, 0.5H), 3.98–3.86 (m, 0.5H), 3.85–3.75 (m, 0.5H), 3.68–3.52 (m, 1H), 3.52–3.38 (m, 1H), 3.23 and 3.21 (2s, 3H), 2.85–2.68 (m, 1H), 2.60–2.46 (m, 2H), 2.08–1.90 (m, 1H), 1.80–1.68 (m, 1H), 1.68–1.40 (m, 3H), 1.12–1.00 (m, 3H), 0.98–0.75 (m, 3H). HRMS (ESI) calcd for $C_{29}H_{35}N_3O_2$ $[M + H]^+$ 458.2802, found 458.2790.

(1R*,2R*)-2-(Pyridin-2-yl)cyclopropanecarboxylic Acid [(2R,3R)-2-Amino-3-methoxybutyl]-(4′-methoxybiphenyl-4-yl)amide (5a).—The procedure for **4h** was followed using 52 mg (0.1 mmol) of **15** and 22.8 mg (0.15 mmol) of 4-methoxyphenylboronic acid to give 32 mg (62% over two steps) of **5a** dihydrochloride (1:1 diastereomeric mixture) as an off-white solid. ^{1}H NMR (300 MHz; CD_3 OD) δ 8.50–8.38 (m, 1H), 8.15–8.00 (m, 1H), 7.60–7.25 (m, 8H), 6.95–6.85 (m, 2H), 4.30–4.18 (m, 0.5H), 4.18–4.05 (m, 0.5H), 3.98–3.85 (m, 0.5H), 3.85–3.72 (m, 0.5H), 3.75 (s, 3H), 3.70–3.52 (m, 1H), 3.52–3.38 (m, 1H), 3.30–3.15 (m, 3H), 2.90–2.78 (m, 1H), 2.10–1.98 (m, 1H), 1.85–1.72 (m, 1H), 1.60–1.45 (m, 1H), 1.12–0.98 (m, 3H). HRMS (ESI) calcd for $C_{27}H_{31}N_3O_3$ $[M + H]^+$ 446.2438, found 446.2431.

(1R*,2R*)-2-(Pyridin-2-yl)cyclopropanecarboxylic Acid [(2R,3R)-2-Amino-3-methoxybutyl]-[4′-(methoxymethyl)biphenyl-4-yl]-amide (5b).—The procedure for 4h was followed using 52 mg (0.1 mmol) of 15 and 24.9 mg (0.15 mmol) of 4-(methoxymethyl)-phenylboronic acid to give 41 mg (77% over two steps) of **5b** dihydrochloride (1:1 diastereomeric mixture) as an off-white solid. ^{1}H NMR (300 MHz; CD_3OD) δ 8.55–8.45 (m, 1H), 8.20–8.15 (m, 1H), 7.78–7.38 (m, 10H), 4.49 (s, 2H), 4.45–

4.30 (m, 0.5H), 4.30–4.15 (m, 0.5H), 4.12–3.95 (m, 0.5H), 3.95–3.80 (m, 0.5H), 3.78–3.62 (m, 1H), 3.62–3.50 (m, 1H), 3.40 (s, 3H), 3.35–3.25 (m, 3H), 3.00–2.82 (m, 1H), 2.20–2.08 (m, 1H), 1.95–1.80 (m, 1H), 1.70–1.55 (m, 1H), 1.22–1.08 (m, 3H). HRMS (ESI) calcd for $C_{28}H_{33}N_3O_3$ $[M + H]^+$ 460.2595, found 460.2579.

(1R,2R)-2-(Pyridin-2-yl)cyclopropanecarboxylic Acid [(2R,3R)-2-Amino-3-methoxybutyl]-[4′-(methoxymethyl)biphenyl-4-yl]amide (6).—The procedure for **4h** was followed using 1.6 g (3.1 mmol) of (1*R*,2*R*)-**15** and 0.77 g (4.65 mmol) of 4-(methoxymethyl)-phenylboronic acid to give 1.05 g (64% over two steps) of **6** dihydrochloride as a white solid: mp 130–132 °C. ^{1}H NMR (300 MHz; CD_3OD) δ 8.40 (br s, 1H), 7.93 (t, J = 7.5 Hz, 1H), 7.67 (d, J = 6.0 Hz, 2H), 7.58 (d, J = 9.0 Hz, 2H), 7.50 (d, J = 6.0 Hz, 2H), 7.42 (d, J = 6.0 Hz, 4H), 4.49 (s, 2H), 4.21 (dd, J = 15.0, 9.0 Hz, 1H), 4.04 (dd, J = 15.0, 6.0 Hz, 1H), 3.60–3.50 (m, 1H), 3.40 (s, 3H), 3.34 (s, 3H), 2.84–2.74 (m, 1H), 2.10–2.02 (m, 1H), 1.85–1.76 (m, 1H), 1.60–1.50 (m, 1H), 1.07 (d, J = 6.0 Hz, 3H) (note: one proton singal overlaps with the CD_3OD solvent peak at δ 3.32–3.30). ^{13}C NMR (75 MHz; $CDCl_3$) δ 174.6, 159.1, 147.0, 142.4, 142.3, 141.8, 140.2, 139.4, 129.6 (two peaks overlap), 129.5, 128.0, 124.2, 124.1, 75.2, 75.0, 58.4, 57.4, 56.9, 51.0, 27.3, 26.6, 17.9, 15.6. HRMS (ESI) calcd for $C_{28}H_{33}N_3O_3$ $[M + H]^+$ 460.2595, found 460.2583.

tert-Butyl {1-[(4′-Propylbiphenyl-4-yl)amino]-2-methyl-propan-2-yl}carbamate (9c).—To a solution of *N*-Boc-2-amino-2-methyl-1-propanol (162 mg, 0.85 mmol) in water-saturated CH_2Cl_2 (5 mL) at room temperature was added Dess–Martin reagent (760 mg, 1.79 mmol), and the reaction was stirred for 1 h. Additional water-saturated CH_2Cl_2 (2 mL) was added every 15 min during the reaction time. The mixture was diluted with Et_2O (30 mL) and poured into a solution of $Na_2S_2O_3$ (1.4 g) in 80% saturated $NaHCO_3$ (30 mL). After stirring for 10 min, the layers were separated and the aqueous layer was extracted with Et_2O (30 mL). The combined organic layers were washed with ice-cold saturated $NaHCO_3$ (10 mL) and water (10 mL). The solution was dried (Na_2SO_4) and concentrated under reduced pressure to give the crude aldehyde **7c**. To a solution of 4-(4′-propylphenyl)aniline (**8b**) (150 mg, 0.71 mmol) in 1,2-dichloroethane (10 mL) was added the above crude aldehyde, followed by $NaBH(OAc)_3$ (301 mg, 1.42 mmol). The mixture was stirred at room temperature overnight. Saturated $NaHCO_3$ (10 mL) was added, and the layers were separated. The aqueous layer was extracted with CH_2Cl_2 (2 × 20 mL). The combined organic layers were washed with brine (3 × 20 mL), dried (Na_2SO_4), and concentrated under reduced pressure. Flash column chromatography of the crude product on silica gel using 0–30% EtOAc in hexanes afforded **9c** (204 mg, 75%) as a white solid: mp 120-122 °C. ^{1}H NMR (300 MHz; $CDCl_3$) δ 7.42–7.38 (m, 4H), 7.20 (d, J = 9.0 Hz, 2H), 6.69 (d, J = 9.0 Hz, 2H), 4.66 (s, 1H), 4.15 (br s, 1H), 3.29 (s, 2H), 2.61 (t, J = 6.0 Hz, 2H), 1.75–1.64 (m, 2H), 1.43 (s, 9H), 1.34 (s, 6H), 0.96 (d, J = 6.0 Hz, 3H). ^{13}C NMR (75 MHz; $CDCl_3$) δ 155.1, 148.0, 140.5, 138.8, 130.3, 128.8, 127.8, 126.2, 113.2, 79.4, 53.2, 52.8, 37.8, 28.5, 28.3, 25.9, 24.7, 14.0. MS (ESI) *m/z* 383.5 $[M + H]^+$.

tert-Butyl {(1S)-2-[(4′-Propylbiphenyl-4-yl)amino]-1-phenylethyl}carbamate (9f).—The procedure for **9c** was followed using 150 mg (0.71 mmol) of **8b** and aldehyde **7f**, prepared by oxidation of *N*-Boc-L-phenylglycinol (203 mg, 0.85 mmol), to give 175 mg

(57%) of **9f** as a white solid: mp 118–120 °C. ^{1}H NMR (300 MHz; $CDCl_3$) δ 7.48–7.30 (m, 9H), 7.20 (d, J = 9.0 Hz, 2H), 6.68 (d, J = 9.0 Hz, 2H), 5.08 (br s, 1H), 4.96 (br s, 1H), 3.94 (s, 1H), 3.50 (d, J = 3.0 Hz, 2H), 2.60 (t, J = 7.5 Hz, 2H), 1.72–1.60 (m, 2H), 1.44 (s, 9H), 0.96 (d, J = 6.0 Hz, 3H). ^{13}C NMR (75 MHz; $CDCl_3$) δ 155.8, 147.1, 140.7, 138.6, 130.9, 128.9, 128.8, 127.9, 126.5, 126.2, 123.4, 80.0, 54.4, 49.8, 37.7, 28.4, 24.6, 14.0. MS (ESI) m/z 431.3 $[M + H]^+$.

tert-Butyl (1-{(4′-Propylbiphenyl-4-yl)-[(1R*,2R*)-2-(pyridin-2-yl)cyclopropanecarbonyl]amino}-2-methyl-propan-2-yl)carbamate (10c).—To a solution of (±)-*trans*-2-(pyridin-2-yl)-cyclopropanecarboxylic acid (78 mg, 0.39 mmol) in CH_2Cl_2 (10 mL) at room temperature was added oxalyl chloride (0.07 mL, 0.78 mmol) and DMF (5 μL). The mixture was stirred at 40 °C for 2 h then cooled to room temperature and concentrated under reduced pressure. The resulting acid chloride was dissolved in CH_2Cl_2 (10 mL) and treated with **9c** (125 mg, 0.33 mmol) and Et_3N (0.18 mL, 1.32 mmol). The mixture was stirred at room temperature overnight. Saturated $NaHCO_3$ (5 mL) was added, and the layers were separated. The aqueous layer was extracted with CH_2Cl_2 (3 × 10 mL). The combined organic layers were washed with brine (3 × 10 mL), dried (Na_2SO_4), and concentrated under reduced pressure. Flash column chromatography of the crude product on silica gel using 0–25% EtOAc in hexanes afforded **10c** (85 mg, 49%) as an oil. ^{1}H NMR (300 MHz; $CDCl_3$) δ 8.28 (d, J = 6.0 Hz, 1H), 7.56–7.38 (m, 5H), 7.30–7.15 (m, 5H), 7.05–6.98 (m, 1H), 5.05 (s, 1H), 4.18–3.98 (m, 2H), 2.66–2.54 (m, 3H), 2.10–1.98 (m, 1H), 1.76–1.60 (m, 3H), 1.50–1.40 (m, 1H), 1.30 (s, 6H), 1.22 (s, 9H), 0.97 (t, J = 6.0 Hz, 3H). ^{13}C NMR (75 MHz; $CDCl_3$) δ 173.5, 159.5, 154.2, 149.2, 142.4, 142.2, 139.9, 137.5, 135.9, 128.9, 128.2, 127.7, 126.8, 122.3, 121.0, 56.6, 54.9, 37.7, 28.3, 28.1, 25.8, 25.6, 25.0, 24.5, 17.6, 13.9. MS (ESI) m/z 529.2 $[M + H]^+$.

tert-Butyl [(1S)-2-{(4′-Propylbiphenyl-4-yl)-[(1R*,2R*)-2-(pyridin-2-yl)cyclopropanecarbonyl]amino}-1-phenylethyl]carbamate (10f).—The procedure for **10c** was followed using 115 mg (0.27 mmol) of **9f** to give 75 mg (49%) of **10f** (1:1 diastereomeric mixture) as an oil. ^{1}H NMR (300 MHz; $CDCl_3$) δ 8.27 (d, J = 6.0 Hz, 1H), 7.60–7.40 (m, 5H), 7.38–7.12 (m, 10H), 7.05–6.95 (m, 1H), 6.05–5.90 (m, 1H), 4.98–4.80 (m, 1H), 4.70–4.50 (m, 1H), 3.50–3.38 (m, 1H), 2.78–2.55 (m, 3H), 2.10–1.98 (m, 1H), 1.80–1.60 (m, 3H), 1.46 and 1.44 (2s, 9H), 1.35–1.20 (m, 1H), 0.97 (t, J = 7.5 Hz, 3H). MS (ESI) m/z 576.7 $[M + H]^+$.

(2S,3R)-2-(Boc-amino)-3-methoxybutyric Acid 4-Bromophenylamide (13).—To a solution of 4-bromoaniline (**8a**) (11.09 g, 64.5 mmol) and *N*-Boc-*O*-methyl-L-threonine (**12**) (15 g, 64.5 mmol) in acetonitrile (300 mL) at room temperature was added DIPEA (16.8 mL, 96 mmol) followed by HBTU (29.3 g, 77.4 mmol). The mixture was stirred overnight, then saturated $NaHCO_3$ (100 mL) was added. The layers were separated. The aqueous layer was extracted with EtOAc (2 × 100 mL). The combined organic layers were washed with brine (3 × 50 mL), dried (Na_2SO_4), and concentrated under reduced pressure. Flash column chromatography of the crude product on silica gel using 0–25% EtOAc in hexanes afforded **13** (22.5 g, 90%) as a white solid: mp 48–50 °C. ^{1}H NMR (300 MHz; $CDCl_3$) δ 8.48 (s, 1H), 7.50–7.40 (m, 4H), 5.55 (s, 1H), 4.40–4.32 (m, 1H), 4.05–3.95 (m, 1H), 3.45 (s, 3H),

1.50 (s, 9H), 1.16 (d, J = 6.0 Hz, 3H). ^{13}C NMR (75 MHz; $CDCl_3$) δ 168.2, 155.9, 136.5, 132.0, 121.6, 117.0, 80.5, 76.2, 57.9, 57.2, 30.9, 28.3, 14.6. MS (ESI) *m/z* 387.3 $[M + H]^+$ (^{79}Br), 389.5 $[M + H]^+$ (^{81}Br).

tert-Butyl {(2R,3R)-1-[(4-Bromophenyl)amino]-3-methoxybutan-2-yl}carbamate (14).—To a solution of **13** (21 g, 54 mmol) in THF (150 mL) at 0 °C was added 1 M borane THF complex solution (162 mL, 162 mmol) over 30 min. The mixture was then stirred at 65 °C for 2 days. After cooling to room temperature, the reaction was quenched with 0.1 N HCl (200 mL) and stirred for 5 min. The solution was basified with saturated $NaHCO_3$. The layers were separated. The aqueous layer was extracted with EtOAc (3 × 150 mL). The combined organic layers were washed with brine (200 mL), dried (Na_2SO_4), and concentrated under reduced pressure. Flash column chromatography of the crude product on silica gel using 0–10% EtOAc in hexanes afforded **14** (6.82 g, 34%) as an oil. ^{1}H NMR (300 MHz; $CDCl_3$) δ 7.23 (d, J = 9.0 Hz, 2H), 6.50 (d, J = 9.0 Hz, 2H), 4.92 (br d, J = 9.0 Hz, 1H), 4.23 (br s, 1H), 3.81–3.71 (m, 1H), 3.58–3.48 (m, 1H), 3.33 (s, 3H), 3.27–3.18 (m, 2H), 1.46 (s, 9H), 1.18 (d, J = 6.0 Hz, 3H). ^{13}C NMR (75 MHz; $CDCl_3$) δ 156.6, 147.4, 131.9, 114.1, 108.5, 79.5, 75.8, 56.4, 54.3, 46.7, 28.4, 15.6. MS (ESI) *m/z* 373.2 $[M + H]^+$ (^{79}Br), 375.0 $[M + H]^+$ (^{81}Br).

tert-Butyl [(2R,3R)-1-{(4-Bromophenyl)-[(1R*,2R*)-2-(pyridin-2-yl)cyclopropanecarbonyl]amino}-3-methoxybutan-2-yl]carbamate (15).—The procedure for **10c** was followed using 2.8 g (7.5 mmol) of **14** to give 3.7 g (95%) of **15** (1:1 diastereomeric mixture) as a yellow foam. ^{1}H NMR (300 MHz; $CDCl_3$) δ 8.35–8.27 (m, 1H), 7.58–7.50 (m, 1H), 7.50–7.38 (m, 2H), 7.25–6.98 (m, 4H), 4.96 (d, J = 9.0 Hz, 1H), 4.35–4.20 (m, 1H), 3.92–3.78 (m, 2H), 3.55–3.45 (m, 1H), 3.45–3.32 (m, 1H), 3.26 and 3.25 (2s, 3H), 2.70–2.62 (m, 0.5H), 2.62–2.55 (m, 0.5H), 2.00–1.88 (m, 1H), 1.72–1.58 (m, 1H), 1.41 (s, 9H), 1.11 and 1.10 (2d, J = 6.0 Hz, 3H). MS (ESI) *m/z* 518.6 $[M + H]$ (^{79}Br), 520.5 $[M + H]^+$ (^{81}Br).

tert-Butyl [(2R,3R)-1-{(4-Bromophenyl)-[(1R,2R)-2-(pyridin-2-yl)-cyclopropanecarbonyl]amino}-3-methoxybutan-2-yl]carbamate ((1R,2R)-15) and tert-Butyl [(2R,3R)-1-{(4-Bromophenyl)-[(1S,2S)-2-(pyridin-2-yl)cyclopropanecarbonyl]amino}-3-methoxybutan-2-yl]-carbamate ((1S, 2S)-15).—The diastereomeric mixture **15** (3.4 g) was separated to (1*R*,2*R*)-**15** (1.62 g, 48%) and (1*S*,2*S*)-**15** (1.61 g, 47%) by preparative HPLC using ChiralPak IA column: mobile phase, 10% 2-propanol/hexanes; flow rate 10 mL/min; detection 220 nm. The diastereomeric excess (de) of both of separated compounds was determined to be >98% by HPLC (ChiralPak IA column; 10% 2-propanol/hexanes; flow rate 1 mL/min; detection 220 nm; retention time, (1*R*,2*R*)-**15** 7.95 min, (1*S*,2*S*)-**15** 12.02 min). (1*R*,2*R*)-**15**: white foam; ^{1}H NMR (300 MHz; $CDCl_3$) δ 8.28 (d, J = 6.0 Hz, 1H), 7.58–7.40 (m, 3H), 7.25–6.98 (m, 4H), 4.98 (d, J = 9.0 Hz, 1H), 4.24 (dd, J = 13.5, 9.0 Hz, 1H), 3.92–3.78 (m, 2H), 3.50 (dd, J = 12.0, 3.0 Hz, 1H), 3.45–3.32 (m, 1H), 3.26 (s, 3H), 2.72–2.62 (m, 1H), 2.00–1.90 (m, 1H), 1.70–1.58 (m, 1H), 1.42 (s, 9H), 1.11 (d, J = 6.0 Hz, 3H); ^{13}C NMR (75 MHz; $CDCl_3$) δ 172.4, 159.1, 156.0, 149.1, 141.4, 135.7, 132.6, 129.7, 122.5, 121.3, 120.9, 78.8, 76.3, 56.4, 53.1, 50.7, 28.2, 27.4, 24.6, 17.7, 15.0; MS (ESI) *m/z* 518.2 $[M + H]^+$ (^{79}Br), 520.4 $[M + H]$

$^{+}$ (^{81}Br). (1*S*,2*S*)-**15**: white foam; ^{1}H NMR (300 MHz; $CDCl_3$) δ 8.29 (d, J = 6.0 Hz, 1H), 7.52 (dd, J = 9.0, 6.0 Hz, 1H), 7.41 (d, J = 9.0 Hz, 2H), 7.20–6.98 (m, 4H), 4.99 (d, J = 9.0 Hz, 1H), 4.28 (dd, J = 13.5, 9.0 Hz, 1H), 3.85–3.75 (m, 2H), 3.49 (dd, J = 13.5, 4.5 Hz, 1H), 3.45–3.32 (m, 1H), 3.25 (s, 3H), 2.65–2.55 (m, 1H), 1.98–1.90 (m, 1H), 1.72–1.62 (m, 1H), 1.41 (s, 9H), 1.10 (d, J = 6.0 Hz, 3H); ^{13}C NMR (75 MHz; $CDCl_3$) δ 172.4, 159.1, 156.0, 149.3, 141.4, 135.8, 132.7, 129.8, 122.4, 121.4, 121.0, 78.9, 76.4, 56.5, 53.2, 50.5, 28.4, 27.7, 24.7, 17.6, 15.0; MS (ESI) *m/z* 518.4 $[M + H]^+$ (^{79}Br), 520.5 $[M + H]^+$ (^{81}Br).

Pharmacology.

Materials.—Cell culture materials were purchased from Fisher SSI. Forskolin was purchased from Sigma-Aldrich. The Lance Ultra kit (TRF0262) was purchased from PerkinElmer.

LanceUltra cAMP Assay Using Stable PPLS-HA-GPR88 CHO Cells.—Stimulation buffer containing 1× Hank's Balanced Salt Solution (HBSS), 5 mM HEPES, 0.1% BSA stabilizer, and 0.5 mM final IBMX was prepared and titrated to pH 7.4 at room temperature. Serial dilutions of the test compounds (5 μL) and 300 nM forskolin (5 μL), both prepared at 4× the desired final concentration in 2% DMSO/ stimulation buffer, were added to a 96-well white ½ area microplate (PerkinElmer). A cAMP standard curve was prepared at 4× the desired final concentration in stimulation buffer, and 5 μL was added to the assay plate. Stable PPLS-HA-GPR88 CHO cells were lifted with versene and spun at 270g for 10 min. The cell pellet was resuspended in stimulation buffer and 4000 cells (10 μL) were added to each well except wells containing the cAMP standard curve. After incubating for 30 min at room temperature, Eu-cAMP tracer and uLIGHT-anti-cAMP working solutions were added per the manufacturer's instructions. After incubation at room temperature for 1 h, the TR-FRET signal (ex 337 nm) was read on a CLARIOstar multimode plate reader (BMG Biotech, Cary, NC).

Data Analysis.—The TR-FRET signal (665 nm) was converted to femtomolar cAMP by interpolating from the standard cAMP curve. Fmol cAMP was plotted against the log of compound concentration and data were fit to a three-parameter logistic curve to generate EC_{50} values (Prism, version 7.0, GraphPad Software, Inc., San Diego, CA).

MDCK Permeability Assay.

MDCK-mdr1 cells obtained from The Netherlands Cancer Institute were grown on Transwell type filters (Corning) for 4 d to confluence in DMEM/F12 media containing 10% fetal bovine serum and antibiotics as has been described previously.[36,37] Compounds were added to the apical side at a concentration of 10 μM in a transport buffer comprising 1× Hank's balanced salt solution, 25 mM D-glucose, and buffered with HEPES to pH 7.4. Samples were incubated for 1 h at 37 °C and carefully collected from both the apical and basal side of the filters. Compounds selected for MDCK-mdr1 cell assays were infused on an Applied Biosystems API-4000 mass spectrometer to optimize for analysis using multiple reaction monitoring (MRM). Flow injection analysis was also conducted to optimize for mass spectrometer parameters. Samples from the apical and basolateral side of the MDCK cell assay were dried under nitrogen on a Turbovap LV. The chromatography was conducted

with an Agilent 1100 binary pump with a flow rate of 0.5 mL/min. Mobile phase solvents were A, 0.1% formic acid in water, and B, 0.1% formic acid in methanol. The initial solvent conditions were 10% B for 1 min, then a gradient was used by increasing to 95% B over 5 min, then returning to initial conditions. Data reported are average values from 2 to 3 measurements.

Solubility Determination.

Thermodynamic solubility was measured in PBS pH 7.4 (Gibco). For each compound, 1.0 mg of powder was combined with 1 mL of buffer to reach a targeted final concentration of 1 mg/mL. The solutions were mixed by repetitive inversion for 24 h at room temperature. Following agitation, the samples were filtrated on Millipore multiscreen polycarbonate membrane (0.4 μm). The eluates were diluted 1000-fold with a mixture of acetonitrile/water (1:1). All samples were assessed in triplicate and analyzed by LC-MS/MS using electrospray ionization against standards prepared in the same matrix. Calibration curve ranged from 1 ng/mL to 2500 ng/mL.

[^{35}S]-GTPγS Binding Assay.

[^{35}S]-GTPγS binding assays were performed on membrane preparations from WT mice or GPR88 KO mice, following our previously published methods.[21,22] To assess [^{35}S]-GTPγS binding in the whole striatal region, brains were quickly removed after cervical dislocation and the whole striatal region was dissected out, frozen, and stored at −80 °C until use. Membranes were prepared by homogenizing brain samples in ice-cold 0.25 M sucrose solution 10 vol (mL/g wet weight of tissue). The obtained suspensions were then centrifuged at 2500*g* for 10 min. Supernatants were collected and diluted 10 times in buffer containing 50 mM TrisHCl (pH 7.4), 3 mM $MgCl_2$, 100 mM NaCl, and 0.2 mM EGTA and then centrifuged at 23000g for 30 min. The pellets were homogenized in 800 μL of ice-cold sucrose solution (0.32 M), aliquoted, and kept at −80 °C. For [^{35}S]-GTPγS binding assays, 2 μg of protein was used per well. Samples were incubated with and without the test compound for 1 h at 25 °C in an assay buffer containing 30 mM GDP and 0.1 nM [^{35}S]-GTPγS. Bound radioactivity was quantified using a liquid scintillation counter. Nonspecific binding was defined as binding in the presence of 10 μM GTPγS; basal binding refers to binding in the absence of the agonist. Data were expressed as a mean percentage of activation above the basal binding. EC_{50} values were calculated using GraphPad Prism software.

Off-Target Selectivity Evaluation.

The off-target profile of RTI-13951-33 was assessed in radioligand binding assays against a panel of 38 GPCRs, ion channels, and transporters at a single concentration of 10 μM by Eurofins PanLabs (Taipei, Taiwan) according to their standard protocols. The full methods and references can be found at: http://www.eurofinsdiscoveryservices.com. The percentage of inhibition was given as the average of two determinations. When significant displacement of radioligand was observed (>50% inhibition at 10 μM), complete concentration-dependent displacement curves (in duplicate) were constructed to generate IC_{50} values. IC_{50} values were determined by a nonlinear regression analysis using MathIQ (ID Business Solutions Ltd., Guildford, Surrey, UK). The equilibrium dissociation constant (K_i) was calculated with

the Cheng–Prusoff equation using the observed IC_{50} of the tested compound, the concentration of radioligand, and the historical values of K_d of the ligand.

Neurotransmitter transporter assays were conducted by NIMH PDSP using Molecular Devices' Neurotransmitter Transporter Uptake Assay Kit (R8174) with HEK293 cells stably expressing human SERT. The full protocol can be found at: http://pdspdb.unc.edu/pdspWeb. In brief, cells were plated in poly-L-Lys (PLL) coated 384-well black clear bottom cell culture plates in DMEM + 1% dialyzed FBS at a density of 15000 cells per well in a total volume of 40 μL. The cells were incubated for a minimum of 6 h before being used for assays. Medium was removed, and 20 μL of assay buffer (20 mM HEPES, 1× HBSS, pH 7.4) was added, followed by 5 μL of 5× drug solutions. The plate was incubated at 37 °C for 30 min. After incubation, 25 μL of dye solution were added and the fluorescence intensity was measured after 30 min at 37 °C using the FlexStation II (bottom read mode, excitation at 440 nm, emission at 520 nm with 510 nm cutoff). Results in relative fluorescence units (RLU) were exported and plotted against drug concentrations in Prism 7.0 for nonlinear regression to obtain IC_{50} values.

Pharmacokinetic Analysis.

A snapshot PK study of RTI-13951-33 was performed using male Long'Evans rats (Paraza Pharma Inc., Montreal, Canada). Doses were formulated in 10% DMSO in saline. On the morning of the PK study, animals were weighed and dosing formulation volumes were calculated accordingly. The compound was injected intraperitoneally to all animals. At selected time points (0.25, 0.5, 1, 2, 4, 8, and 24 h postdose), animals were anesthetized to perform a cardiac puncture to collect blood for pooled plasma analysis, followed by whole body perfusion with phosphate saline buffer (pH 7.4) to wash out any remaining blood from the organs. Brains were harvested and homogenized by polytron 1:4 (w/v) in 25% 2-propanol in water. Brain homogenates were further pooled per corresponding time point and extracted for drug quantification of LC-MS/MS. Samples were prepared and analyzed as follows: Plasma (10 μL) was mixed with 10 μL of 0.5% formic acid in water, 100 μL internal standard working solution (0.1 μM glyburide/labetalol in acetonitrile), vortexed, and centrifuged at 10000g for 25 min at 4 °C. Supernatant (100 μL) was transferred to a 2 mL deep-well plate and diluted with 200 μL of water. Brain homogenate (50 μL) was mixed with 10 μL of 0.5% formic acid in water, 100 μL internal standard working solution (0.1 mM glyburide/labetalol in acetonitrile), vortexed, and centrifuged at 10000g for 25 min at 4 °C. Supernatant (200 μL) was transferred to a 2 mL deep-well plate and diluted with 200 μL of water. LC-MS/MS was conducted using an Applied Biosystems API 4000 HPLC system. Chromatography was performed with an Xbridge BEH C18 (2.1 mm × 30 mm, 2.5 μm) column. Mobile phases were 0.1% formic acid in water (A) and 0.1% formic acid in 25% 2-propanol/acetonitrile (B). Initial conditions were 5% B and held for 0.1 min, followed by a linear gradient to 95% B over 1.4 min. 95% B was held for 2.5 min, followed by a linear gradient to 98% B over 2.55 min. 98% B was held for 3.15 min before returning to initial conditions.

In Vivo Pharmacology.

Self-Administration Training and Testing.—Female Long–Evans rats (Harlan Sprague–Dawley, Indianapolis, IN) were double housed in ventilated cages with water and food available ad libitum in the home cage. The colony room was maintained on a 12-h light/dark cycle, with lights on at 07:00. All experiments were conducted during the light cycle. Animals were under continuous care and monitoring by veterinary staff from the Division of Comparative Medicine (DCM) at UNC—Chapel Hill. All procedures were conducted in accordance with the NIH Guide to Care and Use of Laboratory Animals and UNC—Chapel Hill institutional guidelines. Rats (n = 8 for the alcohol self-administration experiments and n = 7 for the sucrose self-administration experiments) were trained using the same self-administration and training procedures previously described in our publications.[32–34] Self-administration sessions (30 min) took place 5 days/week (M–F) with active lever responses on a fixed ratio 2 (FR2) schedule of reinforcement such that every second response on the lever resulted in delivery of alcohol (0.1 mL) into a liquid receptacle. Responses on the inactive lever were recorded but produced no programmed consequences. Locomotor activity was measured during the self-administration sessions by infrared photobeams that divided the behavioral chamber into four parallel zones. Testing was only conducted following stable self-administration behavior (i.e., defined as no change greater than 15% in the total number of responses during the session prior to testing), and rats had 5 months of alcohol self-administration history prior to testing. Rats received RTI-13951-33 via ip injection 30 min prior to a self-administration session. For each experiment, a repeated measures design was used such that each rat received each dose in a randomized order, with at least one intervening self-administration session between testing days.

Drugs.—The 15% alcohol [v/v] + 2% [w/v] sucrose solution was prepared by dissolving 95% alcohol [v/v] and sucrose in tap water. RTI-13951-33 was dissolved in sterile 0.9% saline to be administered ip at 1 mL/kg.

Data Analysis.—All data were analyzed by one-way repeated-measures analysis of variance (ANOVA) with RTI-13951-33 dose as the within-subjects factor, followed by Tukey posthoc test. Data are represented as means ± SEM, and significance was declared at $p < 0.05$.

Supplementary Material

Refer to Web version on PubMed Central for supplementary material.

ACKNOWLEDGMENTS

This work was supported in part by the National Institute of Mental Health (NIMH, grant MH103708 to C.J.) and National Institute on Alcohol Abuse and Alcoholism (NIAAA, grant no. 16658 to B.K.; grant AA019682 to J.B.), National Institutes of Health, US. V.H.M. was supported by T32NS007431 while working on this project. R.M. was supported by AA023256 (NIAAA) while working on this project. We thank Tiffany Langston and Vineetha Vasukuttan for their valuable technical assistance. The functional data at SERT were generously provided by the National Institute of Mental Health's Psychoactive Drug Screening Program, contract HHSN-271-2013-00017-C (NIMH PDSP). The NIMH PDSP is directed by Bryan L. Roth MD, Ph.D. at the University of North Carolina at Chapel Hill and Project Officer Jamie Driscoll at NIMH, Bethesda MD, USA.

ABBREVIATIONS USED

GPCR	G protein-coupled receptor
2-PCCA	(1*R*,2*R*)-2-(pyridin-2-yl)cyclopropane carboxylic acid ((2*S*,3*S*)-2-amino-3-methylpentyl)-(4′-propylbiphenyl-4-yl)amide
cAMP	cyclic adenosine monophosphate
AUDs	alcohol use disorders
KO	knockout
MSNs	medium spiny neurons
WT	wide-type
CNS	central nervous system
SAR	structure–activity relationship
HBTU	2-(1*H*-benzotriazol-1-yl)-1,1,3,3-tetramethyluronium hexafluorophosphate
THF	tetrahydrofuran
NMR	nuclear magnetic resonance
MS	mass spectrometry
HPLC	high performance liquid chromatography
TLC	thin-layer chromatography
HEK	human embryonic kidney
CHO	Chinese hamster ovary
PPLS	preprolactin leader sequence
HA	human influenza hemagglutinin
TPSA	topological polar surface area
MDCK	Madin–Darby canine kidney
PBS	phosphate-buffered saline
KOR	kappa opioid receptor
VMAT	vesicular monoamine transporter
SERT	serotonin transporter
NIMH	National Institute of Mental Health
ADME	absorption, distribution, metabolism, and excretion

PK	pharmacokinetic
DCM	dichloromethane
DME	1,2-dimethoxyethane
DIPEA	*N,N*-diisopropylethylamine
RLU	relative fluorescence units
FR2	fixed ratio 2

REFERENCES

(1). Rehm J; Mathers C; Popova S; Thavorncharoensap M; Teerawattananon Y; Patra J Global burden of disease and injury and economic cost attributable to alcohol use and alcohol-use disorders. Lancet 2009, 373, 2223–2233. [PubMed: 19560604]

(2). Thavorncharoensap M; Teerawattananon Y; Yothasamut J; Lertpitakpong C; Chaikledkaew U The economic impact of alcohol consumption: a systematic review. Subst. Abuse Treat. Prev. Policy 2009, 4, 20. [PubMed: 19939238]

(3). Lovinger DM; Alvarez VA Alcohol and basal ganglia circuitry: animal models. Neuropharmacology 2017, 122, 46–55. [PubMed: 28341206]

(4). Costardi JV; Nampo RA; Silva GL; Ribeiro MA; Stella HJ; Stella MB; Malheiros SV A review on alcohol: from the central action mechanism to chemical dependency. Rev. Assoc. Med. Bras 2015, 61, 381–387. [PubMed: 26466222]

(5). Cui C; Noronha A; Morikawa H; Alvarez VA; Stuber GD; Szumlinski KK; Kash TL; Roberto M; Wilcox MV New insights on neurobiological mechanisms underlying alcohol addiction. Neuropharmacology 2013, 67, 223–232. [PubMed: 23159531]

(6). Spanagel R Alcoholism: a systems approach from molecular physiology to addictive behavior. Physiol. Rev 2009, 89, 649–705. [PubMed: 19342616]

(7). Bouza C; Magro A; Munoz A; Amate JM Efficacy and safety of naltrexone and acamprosate in the treatment of alcohol dependence: a systematic review. Addiction 2004, 99, 811–828. [PubMed: 15200577]

(8). Heilig M; Goldman D; Berrettini W; O'Brien CP Pharmacogenetic approaches to the treatment of alcohol addiction. Nat. Rev. Neurosci 2011, 12, 670–684. [PubMed: 22011682]

(9). Miller PM; Book SW; Stewart SH Medical treatment of alcohol dependence: a systematic review. Int. J. Psychiatry Med 2011, 42, 227–266. [PubMed: 22439295]

(10). Heilig M; Egli M Pharmacological treatment of alcohol dependence: target symptoms and target mechanisms. Pharmacol. Ther 2006, 111, 855–876. [PubMed: 16545872]

(11). Mizushima K; Miyamoto Y; Tsukahara F; Hirai M; Sakaki Y; Ito T A novel G-protein-coupled receptor gene expressed in striatum. Genomics 2000, 69, 314–321. [PubMed: 11056049]

(12). Van Waes V; Tseng KY; Steiner H GPR88-a putative signaling molecule predominantly expressed in the striatum: cellular localization and developmental regulation. Basal Ganglia 2011, 1, 83–89. [PubMed: 21804954]

(13). Ghate A; Befort K; Becker JA; Filliol D; Bole-Feysot C; Demebele D; Jost B; Koch M; Kieffer BL Identification of novel striatal genes by expression profiling in adult mouse brain. Neuroscience 2007, 146, 1182–1192. [PubMed: 17395390]

(14). Becker JA; Befort K; Blad C; Filliol D; Ghate A; Dembele D; Thibault C; Koch M; Muller J; Lardenois A; Poch O; Kieffer BL Transcriptome analysis identifies genes with enriched expression in the mouse central extended amygdala. Neuroscience 2008, 156, 950–965. [PubMed: 18786617]

(15). Massart R; Guilloux JP; Mignon V; Sokoloff P; Diaz J Striatal GPR88 expression is confined to the whole projection neuron population and is regulated by dopaminergic and glutamatergic afferents. Eur. J. Neurosci 2009, 30, 397–414. [PubMed: 19656174]

(16). Massart R; Mignon V; Stanic J; Munoz-Tello P; Becker JA; Kieffer BL; Darmon M; Sokoloff P; Diaz J Developmental and adult expression patterns of the G-protein-coupled receptor GPR88 in the rat: establishment of a dual nuclear-cytoplasmic localization. J. Comp. Neurol 2016, 524, 2776–2802. [PubMed: 26918661]

(17). Ehrlich AT; Semache M; Bailly J; Wojcik S; Arefin TM; Colley C; Le Gouill C; Gross F; Lukasheva V; Hogue M; Darcq E; Harsan LA; Bouvier M; Kieffer BL Mapping GPR88-Venus illuminates a novel role for GPR88 in sensory processing. Brain Struct. Funct 2018, 223, 1275–1296. [PubMed: 29110094]

(18). Logue SF; Grauer SM; Paulsen J; Graf R; Taylor N; Sung MA; Zhang L; Hughes Z; Pulito VL; Liu F; Rosenzweig-Lipson S; Brandon NJ; Marquis KL; Bates B; Pausch M The orphan GPCR, GPR88, modulates function of the striatal dopamine system: a possible therapeutic target for psychiatric disorders? Mol. Cell. Neurosci 2009, 42, 438–447. [PubMed: 19796684]

(19). Quintana A; Sanz E; Wang W; Storey GP; Guler AD; Wanat MJ; Roller BA; La Torre A; Amieux PS; McKnight GS; Bamford NS; Palmiter RD Lack of GPR88 enhances medium spiny neuron activity and alters motor- and cue-dependent behaviors. Nat. Neurosci 2012, 15, 1547–1555. [PubMed: 23064379]

(20). Meirsman AC; de Kerchove d'Exaerde A; Kieffer BL; Ouagazzal AM GPR88 in A2A receptor-expressing neurons modulates locomotor response to dopamine agonists but not sensorimotor gating. Eur. J. Neurosci 2017, 46, 2026–2034. [PubMed: 28700108]

(21). Meirsman AC; Le Merrer J; Pellissier LP; Diaz J; Clesse D; Kieffer BL; Becker JA Mice lacking GPR88 show motor deficit, improved spatial learning, and low anxiety reversed by delta opioid antagonist. Biol. Psychiatry 2016, 79, 917–927. [PubMed: 26188600]

(22). Meirsman AC; Robe A; de Kerchove d'Exaerde A; Kieffer BL GPR88 in A2AR neurons enhances anxiety-like behaviors. eNeuro 2016, 3, 4.

(23). Ben Hamida S; Mendonca-Netto S; Arefin TM; Nasseef MT; Boulos LJ; McNicholas M; Ehrlich AT; Clarke E; Moquin L; Gratton A; Darcq E; Harsan LA; Maldonado R; Kieffer BL Increased alcohol seeking in mice lacking Gpr88 involves dysfunctional mesocorticolimbic networks. Biol. Psychiatry 2018, 84, 202–212. [PubMed: 29580570]

(24). Jin C; Decker AM; Huang XP; Gilmour BP; Blough BE; Roth BL; Hu Y; Gill JB; Zhang XP Synthesis, pharmacological characterization, and structure-activity relationship studies of small molecular agonists for the orphan GPR88 receptor. ACS Chem. Neurosci 2014, 5, 576–587. [PubMed: 24793972]

(25). Bi Y; Dzierba CD; Fink C; Garcia Y; Green M; Han J; Kwon S; Kumi G; Liang Z; Liu Y; Qiao Y; Zhang Y; Zipp G; Burford N; Ferrante M; Bertekap R; Lewis M; Cacace A; Westphal RS; Kimball D; Bronson JJ; Macor JE The discovery of potent agonists for GPR88, an orphan GPCR, for the potential treatment of CNS disorders. Bioorg. Med. Chem. Lett 2015, 25, 1443–1447. [PubMed: 25754495]

(26). Decker AM; Gay EA; Mathews KM; Rosa TC; Langston TL; Maitra R; Jin C Development and validation of a high-throughput calcium mobilization assay for the orphan receptor GPR88. J. Biomed. Sci 2017, 24, 23. [PubMed: 28347302]

(27). Jin C; Decker AM; Harris DL; Blough BE Effect of substitution on the aniline moiety of the GPR88 agonist 2-PCCA: synthesis, structure-activity relationships, and molecular modeling studies. ACS Chem. Neurosci 2016, 7, 1418–1432. [PubMed: 27499251]

(28). Summerfield SG; Read K; Begley DJ; Obradovic T; Hidalgo IJ; Coggon S; Lewis AV; Porter RA; Jeffrey P Central nervous system drug disposition: the relationship between in situ brain permeability and brain free fraction. J. Pharmacol. Exp. Ther 2007, 322, 205–213. [PubMed: 17405866]

(29). Ghose AK; Herbertz T; Hudkins RL; Dorsey BD; Mallamo JP Knowledge-based, central nervous system (CNS) lead selection and lead optimization for CNS drug discovery. ACS Chem. Neurosci 2012, 3, 50–68. [PubMed: 22267984]

(30). Clark DE; Pickett SD Computational methods for the prediction of 'drug-likeness'. Drug Discovery Today 2000, 5, 49–58.

(31). Hitchcock SA; Pennington LD Structure-brain exposure relationships. J. Med. Chem 2006, 49, 7559–7583. [PubMed: 17181137]

(32). Besheer J; Frisbee S; Randall PA; Jaramillo AA; Masciello M Gabapentin potentiates sensitivity to the interoceptive effects of alcohol and increases alcohol self-administration in rats. Neuropharmacology 2016, 101, 216–224. [PubMed: 26415538]

(33). Jaramillo AA; Randall PA; Stewart S; Fortino B; Van Voorhies K; Besheer J Functional role for cortical-striatal circuitry in modulating alcohol self-administration. Neuropharmacology 2018, 130, 42–53. [PubMed: 29183687]

(34). Randall PA; Stewart RT; Besheer J Sex differences in alcohol self-administration and relapse-like behavior in Long-Evans rats. Pharmacol., Biochem. Behav 2017, 156, 1–9. [PubMed: 28347737]

(35). Randall PA; Jaramillo AA; Frisbee S; Besheer J The role of varenicline on alcohol-primed self-administration and seeking behavior in rats. Psychopharmacology 2015, 232, 2443–2454. [PubMed: 25656746]

(36). Fulp A; Bortoff K; Seltzman H; Zhang Y; Mathews J; Snyder R; Fennell T; Maitra R Design and synthesis of cannabinoid receptor 1 antagonists for peripheral selectivity. J. Med. Chem 2012, 55, 2820–2834. [PubMed: 22372835]

(37). Fulp A; Bortoff K; Zhang Y; Seltzman H; Snyder R; Maitra R Towards rational design of cannabinoid receptor 1 (CB1) antagonists for peripheral selectivity. Bioorg. Med. Chem. Lett 2011, 21, 5711–5714. [PubMed: 21875798]

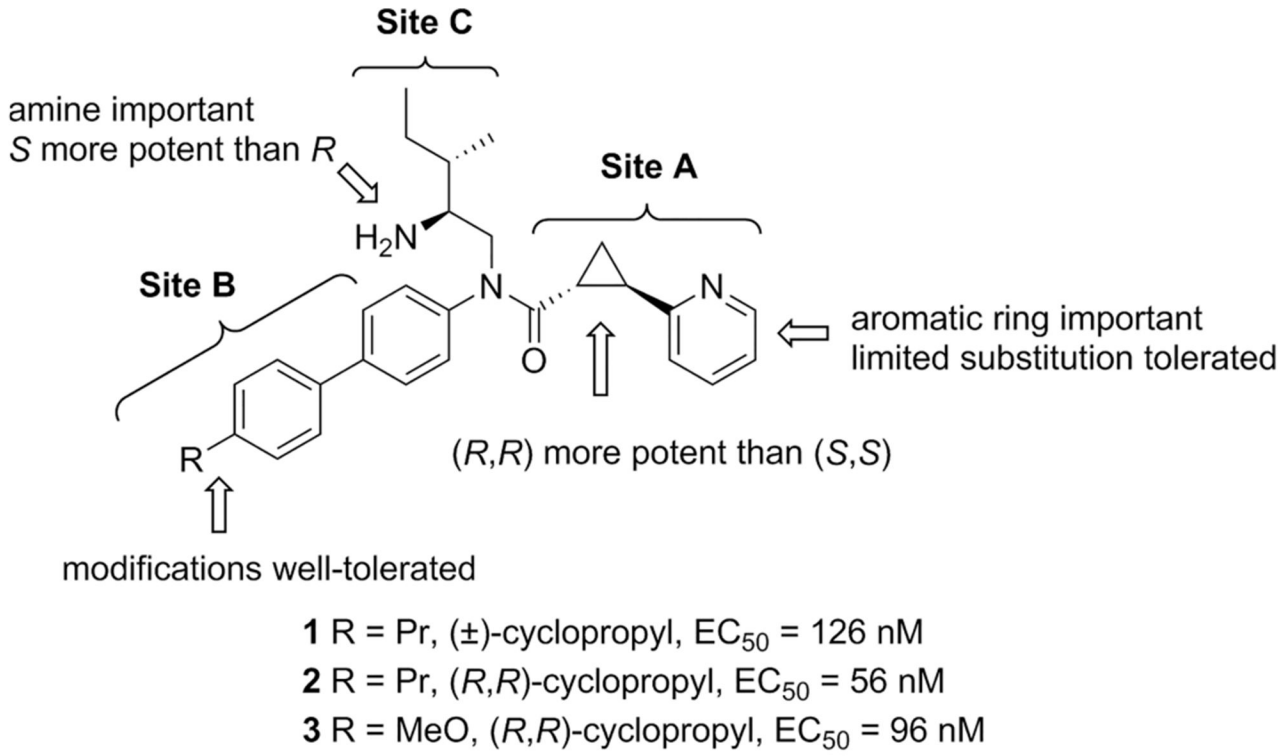

Figure 1.
Structures of 2-PCCA (**1**), (1*R*,2*R*)-2-PCCA (**2**) and **3**, and SAR of sites A–C.

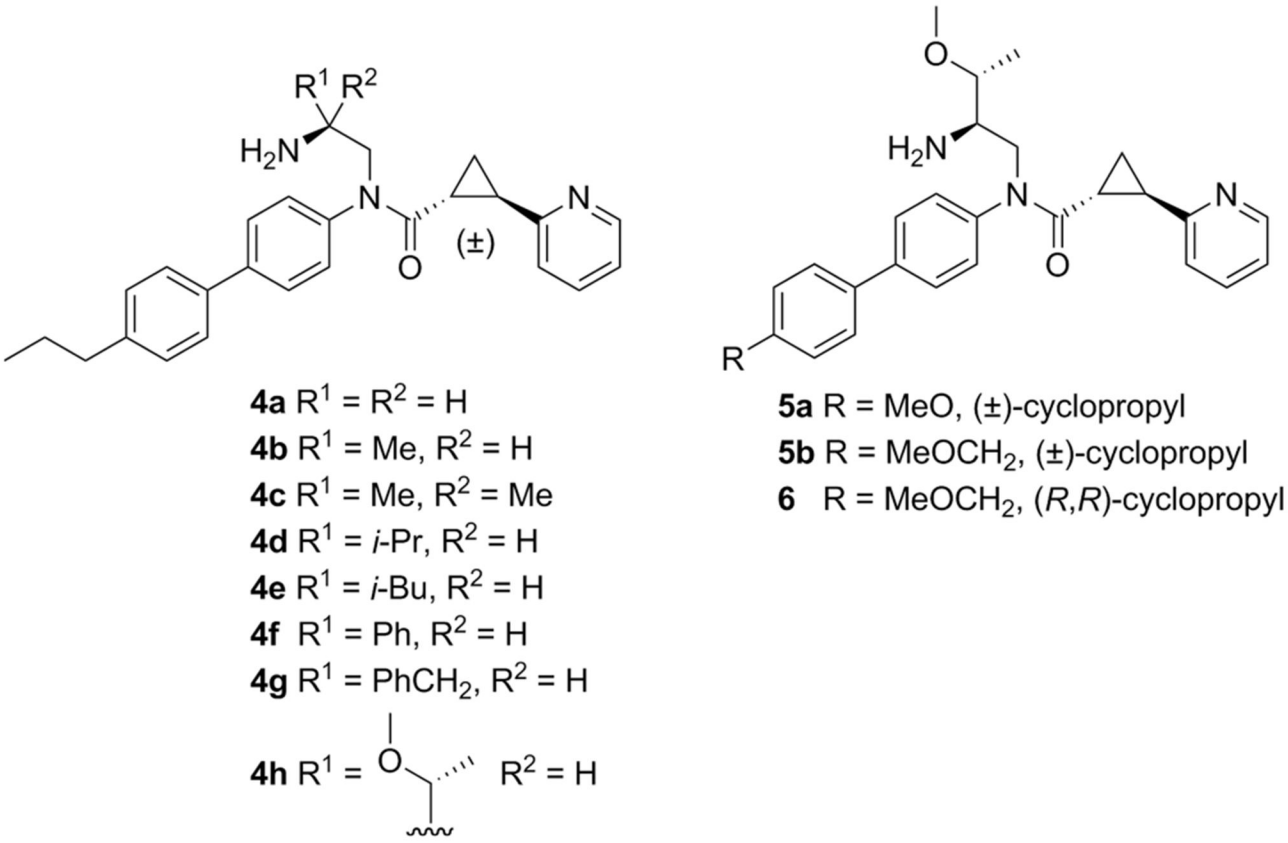

Figure 2.
Structures of 2-PCCA analogues **4a–h**, **5a**, **5b**, and **6**.

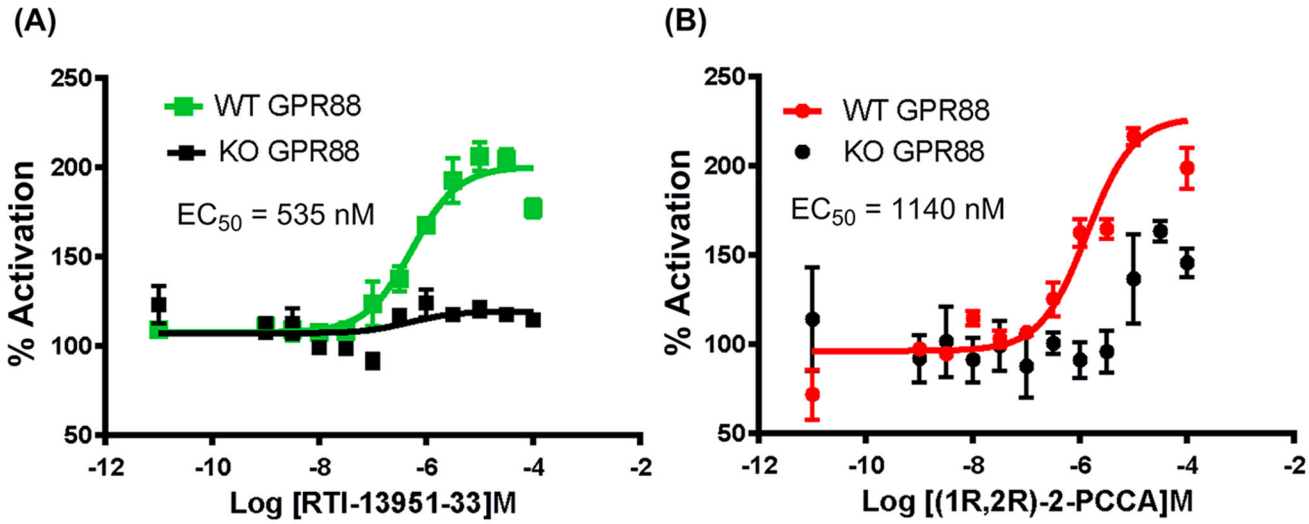

Figure 3.

GTPγS binding of RTI-13951-33 (A) and (1*R*,2*R*)-2-PCCA (B) in mouse striatal membranes vs GPR88 KO mouse striatal membranes. Data points are means ± SEM of two independent experiments run in triplicate.

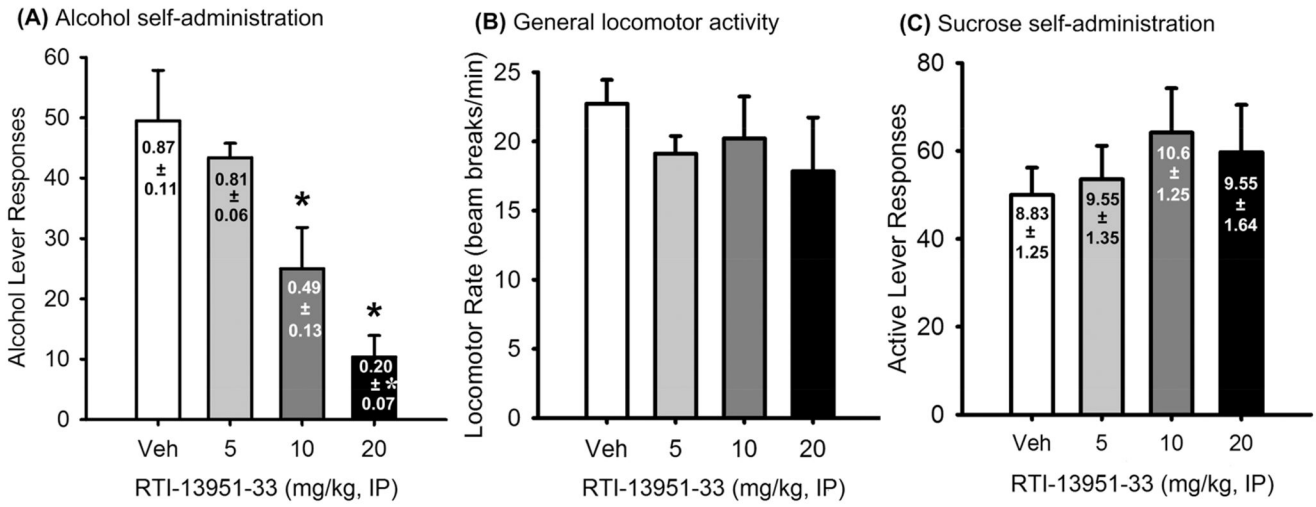

Figure 4.

In vivo activities of RTI-13951-33. (A) In a rat model of alcohol self-administration, RTI-13951-33 significantly reduced alcohol lever responses in a dose–response manner. RM ANOVA: $F_{3,21} = 8.65$, $p < 0.001$. There was also a significant reduction in alcohol intake (g/kg, illustrated on each bar). RM ANOVA: $F_{3,21} = 10.23$, $p < 0.001$, $n = 8$. (B) Locomotor rate measured during the self-administration session was not altered by RTI-13951-33, $n = 8$. (C) In the sucrose self-administration, RTI-13951-33 had no effects on sucrose lever responses and the corresponding sucrose intake (mL/kg, illustrated on each bar), $n = 7$.

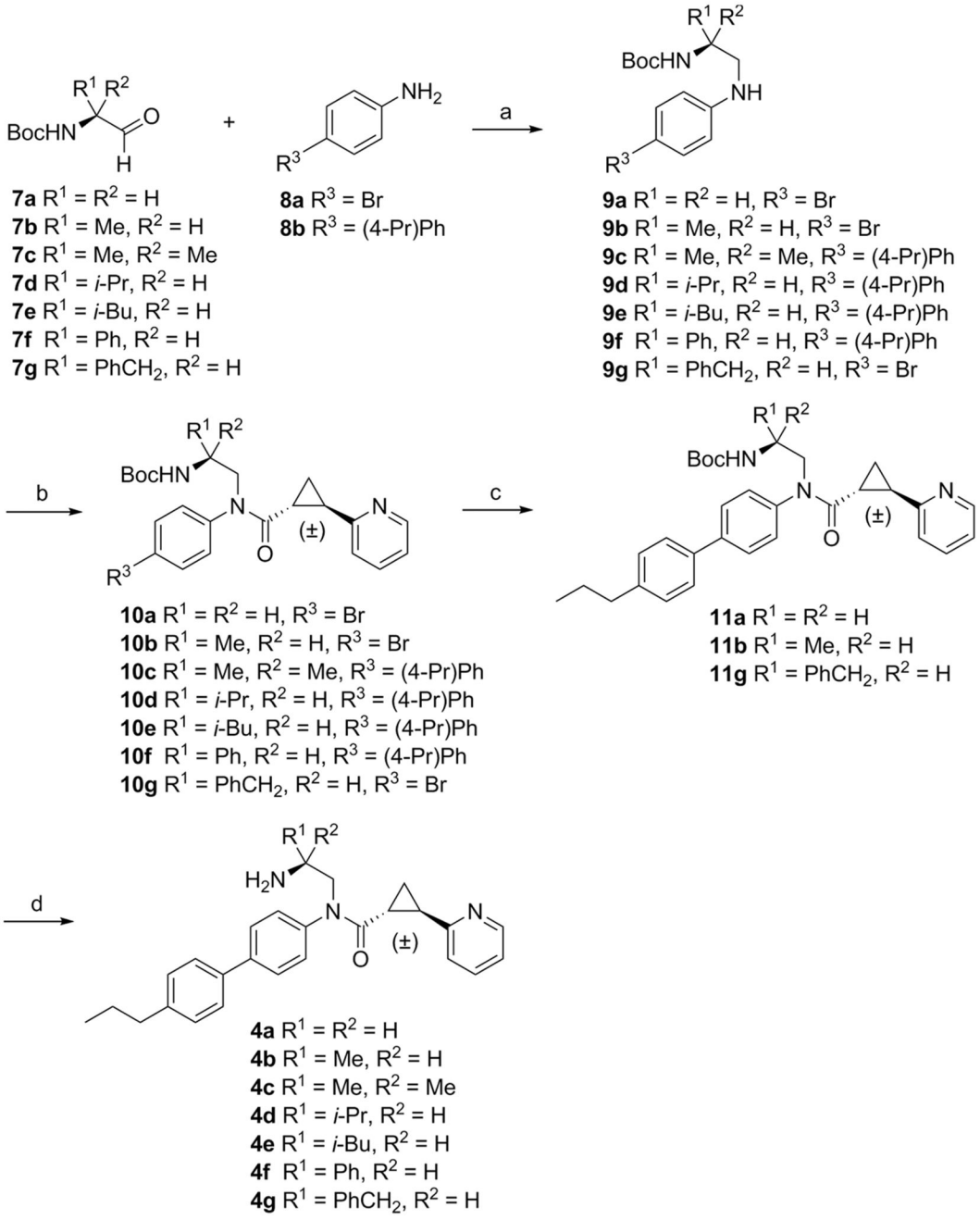

Scheme 1[a]

[a]Reagents: (a) $NaBH(OAc)_3$, 1,2-dichloroethane, rt, overnight; (b) (±)-*trans*-2-(pyridin-2-yl)cyclopropane-carboxylic acid/oxalyl chloride/DCM/40 °C/2 h, concentrated, then **9a–g**/Et_3N/DCM, rt, overnight; (c) 4-propylphenylboronic acid, $Pd(dppf)Cl_2$·DCM, K_3PO_4, DME/H_2O (3:1), microwave, 160 °C, 6 min; (d) 4 M HCl/dioxane, DCM, rt, 6 h.

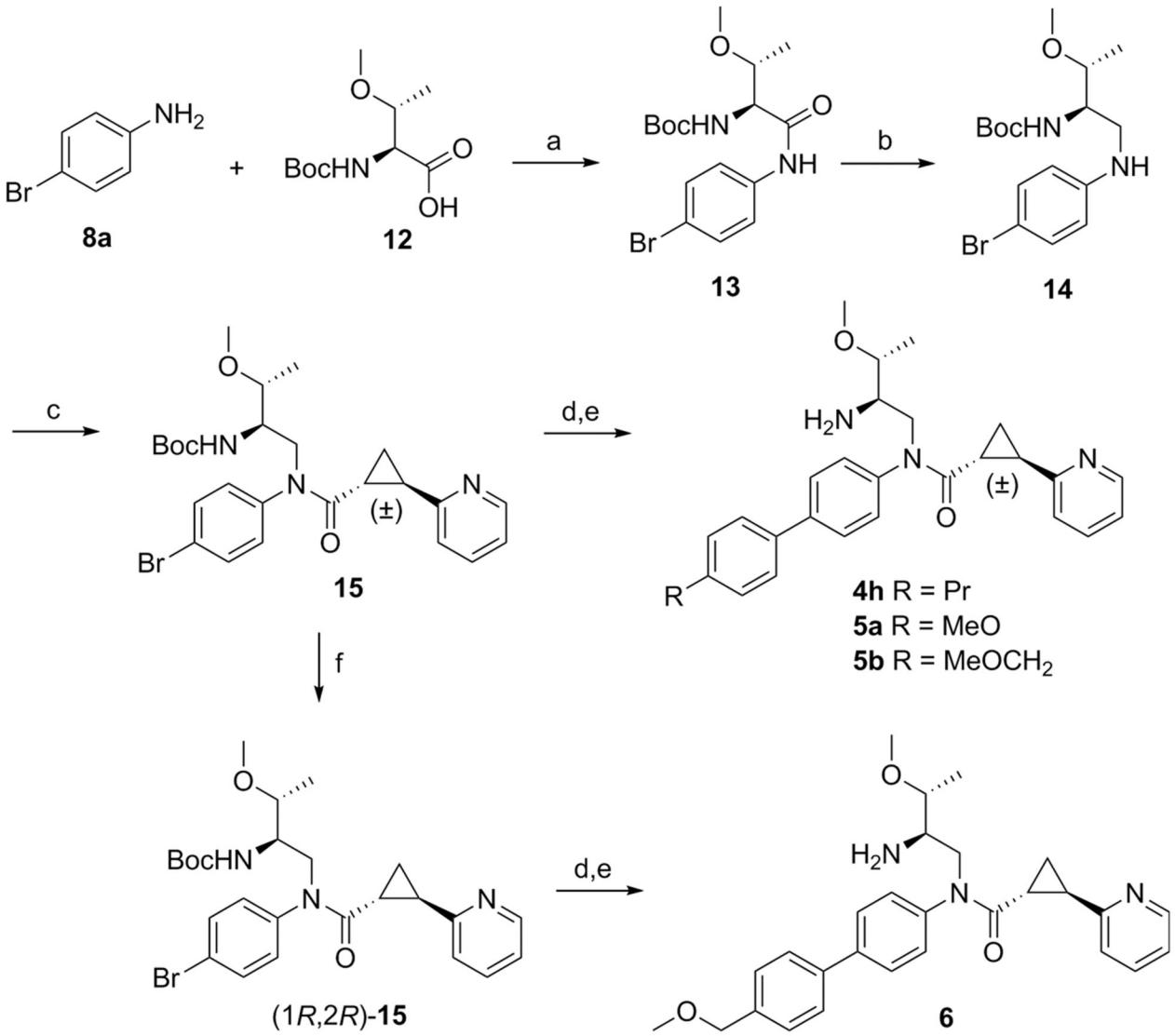

Scheme 2[a]

[a]Reagents: (a) HBTU, DIPEA, MeCN, rt, overnight; (b) BH_3·THF, THF, 65 °C, 2 d; (c) (±)-*trans*-2-(pyridin-2-yl)cyclopropanecarboxylic acid/oxalyl chloride/DCM/40 °C/2 h, concentrated, then **14**/Et_3N/DCM, rt, overnight; (d) arylboronic acid, Pd(dppf)Cl_2·DCM, K_3PO_4, DME/H_2O (3:1), microwave, 160 °C, 6 min; (e) 4 M HCl/dioxane, DCM, rt, 6 h; (f) chiral HPLC separation.

Table 1.

Structures and Activities of Compounds 4a–h, 5a, 5b, and 6

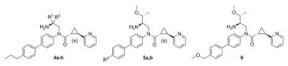

compd[a]	R^1	R^2	R^3	cAMP assay pEC_{50} (EC_{50}, nM)[b]
2-PCCA (**1**)				6.9 ± 0.11 (126)
4a	H	H		6.3 ± 0.07 (501)
4b	Me	H		6.4 ± 0.07 (398)
4c	Me	Me		6.5 ± 0.09 (316)
4d	*i*-Pr	H		6.8 ± 0.02 (158)
4e	*i*-Bu	H		6.9 ± 0.05 (126)
4f	Ph	H		5.9 ± 0.05 (1260)
4g	$PhCH_2$	H		6.3 ± 0.09 (501)
4h	(*R*)-1-methoxyethyl	H		7.2 ± 0.07 (63)
5a			MeO	6.9 ± 0.12 (126)
5b			$MeOCH_2$	7.0 ± 0.09 (100)
6				7.6 ± 0.04 (25)

[a] All compounds were tested as the HCl salt.

[b] pEC_{50} values are means ± standard error of at least three independent experiments performed in duplicate.

Table 2.

Calculated Physiochemical Properties and Preliminary ADME Data

compd	cAMP assay EC_{50} (nM)	clogP[a]	TPSA (Å^2)[a]	log BB	MDCK-mdr1 (%)[b]	solubility (μg/mL)[c]
2	56	6.19	59.22	0.20	1	46.1 ± 1.8
3	96	4.63	68.45	−0.17	8	not determined
4h	63	4.87	68.45	−0.13	3	not determined
6	25	3.34	77.68	−0.50	13	984 ± 9.4

[a] cLogP and TPSA were calculated using Instant JChem 5.4.0 (ChemAxon Ltd.).

[b] Percent transported from the apical (A) to basal (B) side.

[c] Thermodynamic solubility determined in pH 7.4 buffer.

Table 3.

Pharmacokinetic Analysis of RTI-13951-33 in Rat Brain and Plasma (ip, 10 mg/kg)

	plasma	brain	brain/plasma ratio
C_{max} (ng/mL)	874	287	
$t_{1/2}$ (min)	48	87	
AUC_{0-inf} (ng/mL·h)	1510	825	0.5